Aust. J. Phys., 1982, **35**, 543–57

Intermediate-energy Electron Scattering by Atomic Hydrogen

I. E. McCarthy and A. T. Stelbovics

Institute for Atomic Studies, Flinders University of South Australia, Bedford Park, S.A. 5042.

Abstract

Both elastic and inelastic scattering are studied in the framework of the close-coupling equations. The models are formulated in terms of integral equations for T matrices in momentum space. This representation enables one to study the effects of approximations to the multiple-scattering series in a direct manner. For elastic scattering we can thus establish that the approximations made in using a second-order optical-potential formalism give rise to at most a 10% error in the reaction mechanism at 50 eV and considerably less at higher energies. Inelastic 1s–2s and 1s–2p scattering is analysed in terms of a three-state close-coupling model and approximations to it. This enables us to show the marked sensitivity of the angular correlation parameters to approximation and suggests that detailed agreement between theory and experiment requires a close-coupling model containing several more channels.

1. Introduction

The modelling of intermediate-energy electron–hydrogen scattering is still a challenging theoretical problem. In the past few years, extensive experimental investigations have been carried out which have yielded a wealth of detail both for elastic and inelastic scattering from the ground state of atomic hydrogen. Among the more recent studies for elastic scattering we have the experiments of Teubner *et al.* (1974) and the absolute measurements of Williams (1975*a*, 1975*b*) and van Wingerden *et al.* (1977). Inelastic experiments have been performed very recently by several groups. Angular correlations have been measured by Hood *et al.* (1979), Slevin *et al.* (1980), Weigold *et al.* (1980) and Williams (1981). In addition the ratio of the differential cross sections of the 1s–2s and 1s–2p transitions has been measured by Frost and Weigold (1980) and Williams (1981). To date all models lack, to some degree, agreement with experiment.

In principle, a complete theoretical description of the scattering process must couple all excited states of the atom (not only those which are energetically accessible since virtual transitions are possible in intermediate states). One formulation which does this is that of the close-coupling equations. These equations have formed the basis for the most complete and detailed calculations at energies below 50 eV incident electron energy (see e.g. Fon *et al.* 1981). An alternative description of the scattering problem for three particles is given by the Faddeev (1961) equations. Sloan and Moore (1968) showed that the Faddeev equations reduced to the close-coupling form in an on-shell approximation. More recently Redish (1980) has demonstrated more formally that the close-coupling equations can be regarded as being derived from the

Faddeev equations if one redistributes the partitioning of the scattering wavefunction in the internal region. In calculations to date, the close-coupling formalism has proven to be most promising.

In this paper we present a study of the electron–hydrogen scattering at intermediate energies based on the close-coupling formalism. Our primary aim is not so much to attempt to obtain perfect agreement with experiment as to determine the important mechanisms governing elastic and inelastic transitions. The three-state close-coupling model we employ is sufficiently complex to ensure that our conclusions regarding the most sensitive areas of approximation should be valid for more sophisticated calculations.

A novel feature of our calculation is that we have used the Lippmann–Schwinger formulation of the equations and carried out all computations in momentum space. With a single exception (Saha *et al.* 1976) all previous studies have involved solving integro-differential equations in coordinate space and matching appropriate boundary conditions. In contrast, the Lippmann–Schwinger equation for the T matrices is a linear integral equation which has the conditions already built in. In momentum space, the input to the inhomogeneous term and kernel (which are matrices in channel space) are matrix elements that on-shell are the Born–Oppenheimer amplitudes. Since these amplitudes serve as one of the simplest and most widely known models of scattering in atomic physics, the momentum-space close-coupling equations have a direct interpretation as summing the infinite series of multiple scatterings of these amplitudes.

2. Momentum-space Close-coupling Equations

Many reviews of the close-coupling equations have been given in the literature and the reader is referred to these (see e.g. Burke and Smith 1962; Burke and Robb 1975) for a discussion of their derivation in coordinate space and technical details of their solution. Here we use the standard results to write a set of coupled-channels equations for the T-matrix amplitudes based on the analysis of Sloan and Moore (1968).

The Hamiltonian for the electron–hydrogen system is

$$H = K + v_{ep} + v_{ee} + H_T, \tag{1}$$

where H_T is the target (hydrogen atom) Hamiltonian, K is the kinetic energy operator for the incident electron, and v_{ep} and v_{ee} are the Coulomb potentials acting on the incident electron from the target proton and electron respectively. We assume that the proton is static (a very small approximation) so that we can choose for our coordinates the position (or momentum) vectors of the electrons relative to the proton centred at the origin of the coordinate system. The target states which satisfy the equation

$$(\varepsilon_i - H_T)|\phi_i\rangle = 0 \tag{2}$$

form a complete set (i labels discrete and continuum states). The total electron spin of the electron–hydrogen system is conserved, so we can factor it out and antisymmetrize explicitly in terms of singlet (+) and triplet (−) amplitudes. Expanding in terms of the target states we have

$$\langle 1,2|\psi_n^{\pm}\rangle = \sum_i (\langle 1|\phi_i\rangle\langle 2|F_{in}^{\pm}\rangle \pm \langle 2|\phi_i\rangle\langle 1|F_{in}^{\pm}\rangle). \tag{3}$$

The labels 1 and 2 refer to the appropriate particle coordinates (either in position or momentum space).

The $|F_{in}^{\pm}\rangle$ are distorted waves in a single coordinate. Now if we take the Schrödinger equation for $|\psi_n^{\pm}\rangle$:

$$(E-H)|\psi_n^{\pm}\rangle = 0, \tag{4}$$

and fold on the left with $\langle\phi_j|$ we obtain the close-coupling equations upon expanding in terms of equation (3):

$$\sum_i \{(E-\varepsilon_j-K)\delta_{ij}-V_{ji}^{\pm}(E)\}|F_{in}^{\pm}\rangle = 0. \tag{5}$$

The potentials are given by

$$\begin{aligned} V_{ji}^{\pm}(E) &= \langle\phi_{1j}|v_{ep}+v_{ee}|\phi_{1i}\rangle \pm \langle\phi_{2j}|\varepsilon_i+\varepsilon_j-E+v_{ee}|\phi_{1i}\rangle \\ &= V_{ji}^{D} \pm V_{ji}^{E}. \end{aligned} \tag{6}$$

(We use the subscript 1 or 2 on the target states to denote the channels obtained by forming the target states with electron 1 or 2.) If we impose the boundary condition that the initial asymptotic state from which $|\psi_n^{\pm}\rangle$ develops is the product of a plane wave $|\boldsymbol{k}'\rangle$ and the target state $|\phi_n\rangle$, the scattering amplitude from an initial state n to a final state m is

$$\langle\boldsymbol{k}|T_{mn}^{\pm}(E+\mathrm{i}0)|\boldsymbol{k}'\rangle = \sum_l \langle\boldsymbol{k}|V_{ml}^{\pm}(E)|F_{ln}^{\pm}\rangle, \tag{7}$$

where the momenta k and k' are related to the total energy E by the relation

$$E = \tfrac{1}{2}k^2+\varepsilon_m = \tfrac{1}{2}k'^2+\varepsilon_n. \tag{8}$$

One can then straightforwardly recast equation (5) into a Lippmann–Schwinger equation for the T-matrix amplitudes:

$$T_{mn}^{\pm}(E+\mathrm{i}0) = V_{mn}^{\pm}(E+\mathrm{i}0) + \sum_l V_{ml}^{\pm}(E+\mathrm{i}0)\,G_0(E-\varepsilon_l+\mathrm{i}0)\,T_{ln}^{\pm}(E+\mathrm{i}0), \tag{9}$$

where

$$G_0(W) = (W-K)^{-1}. \tag{10}$$

The sum over l implies a summation over all target states including the continuum. However, in practical applications one projects the infinite set of equations onto a restricted space of channels by means of a Feshbach projection. If we are interested in transitions between a set of states of the target $m_1, \ldots, m_p$ we define a projection operator P such that

$$\begin{aligned} Pm &= m, \quad \text{if } m \in m_1, \ldots, m_p \\ &= 0, \quad \text{otherwise}, \end{aligned} \tag{11a}$$

and a corresponding operator Q where

$$\begin{aligned} Qm &= 0, \quad \text{if } m \in m_1, \ldots, m_p \\ &= m, \quad \text{otherwise}. \end{aligned} \tag{11b}$$

Then from the standard properties $P+Q = 1$, $PQ = QP = 0$, $P^2 = P$ and $Q^2 = Q$ one gets on application of the projection onto equation (9)

$$PT^{\pm}P = Z^{\pm} + Z^{\pm}G_0 PT^{\pm}P, \tag{12}$$

with

$$Z^{\pm} = PV^{\pm}P + PV^{\pm}QG^{\pm}(E+\mathrm{i}0)QV^{\pm}P, \tag{13}$$

and where $QG^{\pm}Q$ satisfies the integral equation

$$QG^{\pm}Q = G_0 Q + G_0 QV^{\pm}QG^{\pm}Q. \tag{14}$$

It must be remembered that $V^{\pm}$ and $Z^{\pm}$ are energy dependent. For brevity we omit explicitly writing this dependence in future.

All calculations of electron–hydrogen scattering involve solving equation (12) with some approximation to $Z^{\pm}$, the effective potential. If we choose to project only onto the elastic channel, i.e. $m_p = 1$, the effective potential is called the optical potential. We now turn to the approximations which we wish to consider in our numerical calculations.

3. Multichannel Models

Three-state Model

The basic model which we choose as our reference in order to test the validity of some simpler models and the importance of various groups of terms in the multiple-scattering series is the three-state close-coupling model. In this model one defines $P = P_{(3)} = 1\mathrm{s}, 2\mathrm{s}, 2\mathrm{p}$ and approximates $Z^{\pm}$ by $Z^{\pm}_{(3)} \approx P_{(3)} V^{\pm} P_{(3)}$. In effect we have made the assumption that $Q_{(3)} G Q_{(3)} = 0$. For incident energies above 50 eV the three-state model is currently the most sophisticated level of close-coupling equation to be solved for e–H scattering.

Second-order Model

In the case of intermediate-energy scattering the elastic amplitude is most commonly modelled by choosing $P = P_{(1)} = 1\mathrm{s}$, and making the approximation $QG^{\pm}Q = G_0 Q$. This can be seen to be equivalent to retaining the term of order E^{-1} in equation (14) and neglecting terms of order E^{-2} or greater; thus

$$Z^{\pm}_{(1)} \approx V^{\pm}_{1\mathrm{s},1\mathrm{s}} + \sum_{q \neq 1\mathrm{s}} V^{\pm}_{1\mathrm{s},q} G_0(E-\varepsilon_q+\mathrm{i}0) V^{\pm}_{q,1\mathrm{s}}. \tag{15}$$

The second-order part of this is called the polarization potential.

This approximation describes the elastic channel rather well at intermediate energies. We will discuss the reason for this in Section 5.

Unitarized-Born Approximations (UBA)

At intermediate and high energies one often uses an approximation based on the representation of the free Green function as

$$G_0(E-\varepsilon_q+\mathrm{i}0) \sim -\mathrm{i}\pi\delta(E-\varepsilon_q-K). \tag{16}$$

When we are solving equation (12) for the transition amplitudes we can choose to make this approximation in one or more channels at a time. In practice one would in the first instance confine its use to those channels which do not contribute a major

part to the reaction mechanism. Its utility lies in the fact that after partial wave analysis the delta-function integration can be performed explicitly. This gives a simple algebraic coupling to the channel approximated in this way (which in turn enables a large number of channels to be included if so desired).

We note in passing that this type of approximation occurs naturally in the representation of the T matrices by equation (12); with the standard solution of the close-coupling equations, in the coordinate representation through use of equation (5) with matching boundary conditions, there is no ready analogue to it.

4. Numerical Considerations

After performing a partial wave analysis of equation (9), the equations one has to solve numerically reduce to the form

$$T_{mn}^{(J)\pm}(k,k') = V_{mn}^{(J)\pm}(k,k') + \sum_l \int_0^\infty \mathrm{d}k''\, k''^2\, V_{ml}^{(J)\pm}(k,k'') \times \frac{1}{E-\varepsilon_l-\frac{1}{2}k''^2+\mathrm{i}0}\, T_{ln}^{(J)\pm}(k'',k'). \tag{17}$$

This is a Fredholm equation of the second kind and there are standard methods for solving it. One replaces the integral by a numerical quadrature rule with quadrature points k_i. The integral equation then reduces to a matrix equation. A nice exposition of the technique is given by Mayers (1974). Treatment of the singularity in the kernel Green function is also straightforward. One simply uses the identity

$$\mathrm{P}\int_0^\infty \frac{\mathrm{d}k''}{E-\varepsilon_l-\frac{1}{2}k''^2} = 0$$

to subtract out the singularity. As explained by Mayers one obtains a slightly modified matrix equation to solve.

The calculation of the matrix elements $V_{mn}^{(J)\pm}(k,k')$ presents little problem. All the direct Born matrix elements $V_{mn}^{\mathrm{D}}(\boldsymbol{k},\boldsymbol{k}')$ can be calculated analytically. The partial-wave-analysed matrix elements can be reduced to the computation of a set of recurrence relations. The full expressions for transitions involving 1s, 2s and 2p channels are given by Lawson *et al.* (1961) and we shall not repeat them here. The calculation of the exchange parts of the amplitudes is more complicated. In general their calculation can be reduced to one of performing a single integration by numerical quadrature.

One point which deserves comment is how the partial wave equations serve to eliminate a problem which arises in the full three-dimensional version of the equations. In the direct part of the potential, the dipole matrix elements ($V_{1\mathrm{s},2\mathrm{p}}^{\mathrm{D}}$ and $V_{2\mathrm{s},2\mathrm{p}}^{\mathrm{D}}$ for example) take the form

$$V_{n\mathrm{s},n'\mathrm{p}}^{\mathrm{D}}(\boldsymbol{k},\boldsymbol{k}') = \mathrm{Y}_{1m}(\boldsymbol{Q})\, g(Q^2)/Q,$$

with

$$\boldsymbol{Q} = \boldsymbol{k}'-\boldsymbol{k}.$$

Because $g(0)$ is finite the kernel has a weak singularity at $\boldsymbol{k} = \boldsymbol{k}'$. Treatment of this singularity and its relation to the long-range behaviour of the polarization potential has been discussed by McCarthy *et al.* (1981*b*). However, since the singularity

is of order Q^{-1} one finds after a partial wave analysis that $V^{(J)D}_{ns,n'p}(k,k')$ is finite in the limit $k = k'$.

As an initial test of our numerical procedures equation (17) was solved using the UBA approximation (16) in all channels and neglecting the exchange potentials. The results agreed perfectly with those of Burke and Seaton (1961). The exchange matrix elements were checked by calculating the differential cross sections corresponding to $V^{\pm}_{nl,n'l'}(\boldsymbol{k},\boldsymbol{k}')$ (the Born–Oppenheimer amplitudes), with k and k' given by the on-shell condition (8). They agree with those of Mott and Massey (1965).

The full equations were solved using up to 32 quadrature points per channel. As J increases one notes two things. Firstly, the effects of exchange become smaller. At $J = 15$ and intermediate energies, the exchange potentials give rise to at most 2% differences when compared with the direct potentials alone. Secondly, the solution of the full close-coupling equations is approximated very closely by the pure UBA model after $J = 26$. Thus in all our calculations we solved the equations with exchange up to and including $J = 15$. From $J = 15$ to 26 we solved the equations with the direct potential only. From $J = 27$ to 50 we used the UBA approximation. The contribution for all higher J was taken into account by analytic formulae for the Born matrix elements.

We further tested our numerical procedures by making extensive comparisons with the close-coupling calculations of Burke and Schey (1962), Burke *et al.* (1963) and Kingston *et al.* (1976). Our results are in reasonable agreement. This is in contrast to the work of Saha *et al.* (1976) which exhibits significant disagreement for low partial waves.

5. Results and Discussion

All the calculations were carried out at the two intermediate energies 54·46 and 100 eV for which a large amount of experimental data is available.

Elastic Scattering

In Table 1 we show the results for the differential cross section obtained by solving the three-state close-coupling equations at 100 eV. We note that in this model, all possible terms due to rescattering in the 1s, 2s and 2p channels are summed to all orders by solving equation (12). Thus, for example, we have terms of the type $V_{1s2s}(G_0 V_{2s2s})^n G_0 V_{2s1s}$ and $V_{1s2p}(G_0 V_{2p2p})^n G_0 V_{2p1s}$, which are not incorporated in the second-order optical potential of equation (15) or the multiple-scattering series it generates from equation (12). One can test the effect of neglecting these terms by restricting the momentum-space sum in the second-order potential to the 2s and 2p states. When we do this we get the second-order potential approximation to the three-state close-coupling calculation. It can be seen from Table 1 that this is an excellent approximation at 100 eV, as the maximum difference in the cross sections is less than 5% at all angles. Generally at very forward angles the difference is greatest. What this comparison between the two models tells us is that the dominant scattering mechanism consists of all terms where excitation to the 2s or 2p state is followed by a transition to the ground state. Having realized this one can then examine the relative importance of the 2s and 2p states in the scattering. We have done this by carrying out the second-order calculation in which the 1s state is coupled to the 2p only. If we compare the two-state second-order result with the three-state one, we

Table 1. Differential elastic and total elastic cross sections for e–H scattering at 100 eV

The units are a_0^2 and the notation $-x$ indicates $\times 10^{-x}$. The experimental cross sections are those of Williams (1975*a*, 1975*b*); the numbers in brackets referring to the error in the last two significant figures of the data. The columns labelled 1s–2s–2p and 1s–2p are three- and two-state close-coupling models. The columns labelled 2nd order refer to the equivalent optical-potential approximations. The column labelled 2nd order opt. is an equivalent local approximation to the optical potential. See text for further details

θ (deg.)	Exp.	Cross section 1s–2s–2p (full)	1s–2s–2p (2nd order)	1s–2p (2nd order)	1s–2s–2p (2nd order opt.)
0		2·62	2·74	2·64	
5		1·96	2·05	—	1·92
10		1·21	1·27	1·22	1·24
20	1·10(10)	0·708	0·723	0·707	0·72
30	0·509(49)	0·398	0·397	0·392	0·40
40	0·288(27)	0·214	0·212	0·211	0·21
50	0·132(12)	0·119	0·119	0·119	0·115
60	0·0722(71)	0·717−1	0·715−1	0·724−1	0·67−1
70	0·0491(46)	0·452−1	0·452−1	0·460−1	0·42−1
80	0·0295(30)	0·299−1	0·301−1	0·307−1	0·28−1
90	0·0209(20)	0·210−1	0·215−1	0·220−1	0·20−1
100	0·155−1(15)	0·159−1	0·163−1	0·167−1	0·15−1
110	0·115−1(12)	0·125−1	0·128−1	0·131−1	0·117−1
120	0·92−2(9)	0·995−2	0·103−1	0·106−1	0·95−2
130	0·78−2(7)	0·833−2	0·880−2	0·902−2	0·80−2
140	0·65−2(7)	0·739−2	0·782−2	0·800−2	0·69−2
150		0·671−2	0·708−2	0·725−2	—
160		0·608−2	0·653−2	0·668−2	0·57−2
170		0·564−2	0·625−2	0·639−2	—
180		0·655−2	0·643−2	0·650−2	0·54−2
σ_E	1·75	1·246	1·246	1·252	1·225

notice that the omission of scattering to the 2s state accounts at most for a 2% error. In the forward direction the error brings the two-state calculation into better agreement with the full three-state close-coupling answers. The errors one makes in using more than one approximation tend to cancel to some extent. This is a pattern we find repeated in other results.

Thus at 100 eV we may summarize our findings as follows. The reaction mechanism to better than 90% agreement in the elastic cross section is governed by multiple rescatterings in the elastic channel and dipole transitions to and from the elastic channel. Rescatterings in the inelastic channels have small effects (<10%) which are most noticeable at backward angles.

In Table 1 (last column) we have also shown the results of a second-order optical potential calculation where the polarization potential has been calculated in a spherically averaged equivalent local approximation. This type of approximation was used by McCarthy *et al.* (1981*a*) to include contributions from higher dipoles due to 3p, 4p and 5p excitation in an explicit second-order optical-model calculation. One sees that it provides a good representation of the full close-coupling cross section.

Table 2. Differential elastic and total elastic cross sections for e–H scattering at 54·46 eV

For details see notes to Table 1

θ (deg.)	Cross section			
	1s–2s–2p (full)	1s–2s–2p (2nd order)	1s–2p (full)	1s–2p (2nd order)
0	3·72	3·98	3·68	3·85
10	2·00	2·14	1·98	2·06
20	1·115	1·20	1·14	1·16
30	0·736	0·754	0·743	0·736
40	0·474	0·476	0·485	0·471
50	0·307	0·305	0·319	0·305
60	0·202	0·201	0·213	0·203
70	0·136	0·136	0·146	0·140
80	0·956−1	0·967−1	0·103	0·100
90	0·702−1	0·722−1	0·768−1	0·751−1
100	0·539−1	0·565−1	0·595−1	0·591−1
110	0·429−1	0·459−1	0·476−1	0·482−1
120	0·353−1	0·385−1	0·394−1	0·406−1
130	0·301−1	0·336−1	0·337−1	0·354−1
140	0·266−1	0·302−1	0·298−1	0·319−1
150	0·242−1	0·278−1	0·271−1	0·294−1
160	0·225−1	0·262−1	0·253−1	0·278−1
170	0·216−1	0·253−1	0·243−1	0·269−1
180	0·215−1	0·252−1	0·241−1	0·268−1
σ_E	2·599	2·680	2·674	2·658

The conclusions drawn from the 100 eV models remain valid at 54·46 eV. From Table 2 one observes that the second-order approximation reproduces the mid-angle cross section well. At very forward angles ($\lesssim 10°$) it overshoots by about 7%; at backward angles it eventually becomes 20% too large. Again if we omit coupling to the 2s channel we see that both the two-state close-coupling calculation and the corresponding second-order one account for 80% of the cross section. Thus the 54·46 eV results show a similar trend to those for 100 eV but with more pronounced disagreement. This is of course due to the fact that the approximation we made in representing the Q-space Green function of equation (14) by the first term becomes less reliable as the energy is decreased.

From the analysis we have carried out we can estimate the errors associated with more sophisticated second-order calculations which have been used to describe elastic scattering at intermediate energies. In these calculations one makes a compromise by using a second-order potential so that rescattering effects in Q space are neglected. However, one is able to include the effect of the dipole transitions to the excited and continuum states in Q space by using a closure approximation (see e.g. Byron and Joachain 1981) or by using explicit calculation over all significant states as has been done by McCarthy *et al.* (1981*a*). This brings the forward cross section up significantly and at the same time reduces it in the backward direction. The net effect at 100 eV in the McCarthy *et al.* calculation is to drag the cross section about 25% below the experimental values. Thus if we return to Table 1 and look at the second-order potential result with a Q space consisting of only the 2s and 2p states we see that taking account of the higher dipole contributions is quite significant; from being

20% too large at 140° it becomes 20% too small. As we have estimated the approximations inherent in the method to be of the order of 5% at this energy the discrepancy between theory and experiment is not readily explained. Two other recent calculations, those of Scott and Bransden (1981) and a distorted-wave model of the second-order potential by Kingston and Walters (1980), reach similar conclusions.

At the lower energy of 50 eV there are available the six-state close-coupling results of Fon *et al.* (1981). They include the 2s and 2p states as well as three pseudo-states. These are variationally determined states chosen to take account of the neglected dipole transitions. The agreement at forward angles is still poor, although it is excellent at backward angles. All the second-order theories, with the exception of Byron and Joachain (1981), do considerably better at 50 eV than at 100 eV. The agreement with experiment is good at forward angles. At backward angles the theory answers tend to lie slightly below the experimental points. Since we have estimated the errors in the approximations inherent in the second-order potential results to be up to 20% at backward angles for 54·46 eV, the agreement with experiment is very satisfactory.

Inelastic Scattering

In contrast to elastic scattering, the theoretical description of inelastic 1s–2s and 1s–2p scattering is far from complete. All models have significant disagreement with experiment for the angular correlation parameters. Also the ratio of the 1s–2s and 1s–2p differential cross sections is predicted badly by all theories with the exception of the three-state close-coupling model. What this indicates is that the multiple-scattering series terms which dominate inelastic scattering are much more sensitive to approximation than those for elastic scattering. In order to ascertain which terms the inelastic amplitude is most sensitive to we again use the three-state close-coupling equations as our basic model and make a variety of approximations to them.

First we look at the ratio of the inelastic differential cross sections for the 1s–2s and 1s–2p transitions, which we write as $\sigma(2s)/\sigma(2p)$. The approximations one can make rather straightforwardly are to use the UBA in either the 2s or 2p channels. From equation (16) this means that we approximate G_0 by its imaginary part. Although we are thus including all three channels, computationally the UBA reduces the problem to an effective two-channel coupling. The coupling to the UBA parametrized channel amounts to including one extra row and column in the discretized matrix equation. In Fig. 1 we show $\sigma(2s)/\sigma(2p)$ at an energy of 54·46 eV for the three-state model and the two UBA parametrizations. The experimental data are those of Williams (1981) and Frost and Weigold (1980). As Frost and Weigold have pointed out, agreement with the three-state close-coupling calculation of Kingston *et al.* (1976) is excellent. They also discussed the other models which fail to predict the ratio at all well (the interested reader is referred to their paper for a discussion). We note also the impressive agreement of the Williams (1981) data with theory.

If we look at the two UBA curves it is obvious that the 2s–2p ratio is very sensitive to the nature of the approximation at angles $\gtrsim 40°$. By neglecting the real part of the Green function in the 2p channel we apparently seriously underestimate the contribution of the multiple-scattering terms involving $V_{2p2p}\,G(E+\varepsilon_{2p}+i0)$ at backward angles. Thus $\sigma(2p)$ is far too small (see dot–dash curve in Fig. 2). However, $\sigma(2s)$ is far less sensitive to the UBA approximation in the 2p channel, which results in the ratio $\sigma(2s)/\sigma(2p)$ being much too large at backward angles (it peaks at a value of ≈ 7 at 120°). Similar considerations apply to the UBA in the 2s channel. Here

$\sigma(2s)$ is underestimated at backward angles, while $\sigma(2p)$ is modified much less (see dotted curve in Fig. 2), resulting in a ratio $\sigma(2s)/\sigma(2p)$ which is too small throughout the entire angular range. One observation we can make from the two model calculations is that since the UBA is an approximation which is good at high energies all three curves should approach each other. That they do not is a clear indication that 54·46 eV is too low an energy to assume that intermediate virtual rescatterings proceed dominantly on the energy shell. This does not mean UBA approximations are not useful at this energy, merely that one must use them with some caution.

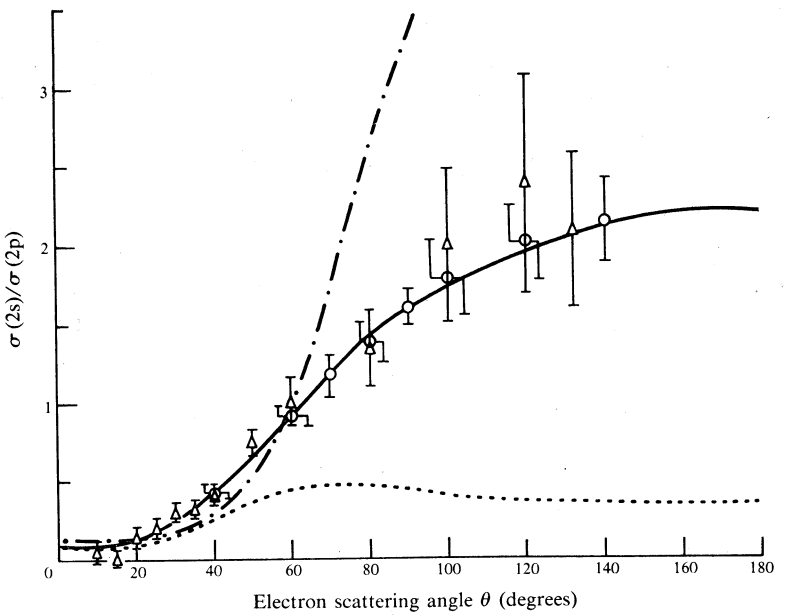

Fig. 1. Ratio of inelastic differential cross sections $\sigma(2s)/\sigma(2p)$ at $E = 54{\cdot}46$ eV. Theory: solid curve, 1s–2s–2p (full three-state close coupling); dotted curve, 1s–2s(UBA)–2p (UBA used in 2s channel); dot–dash curve, 1s–2s–2p(UBA) (UBA used in 2p channel). Experiment: circles, Williams (1981); triangles, Frost and Weigold (1980)

A good illustration of this is provided by the $\sigma(2p)$ inelastic cross section which we have calculated for four approximations in Fig. 2. We see that the three-state close-coupling model gives a cross section in good agreement with the Williams (1981) absolute results. One might guess that to a first approximation most of the reaction mechanism might be contained in coupling the 1s and 2p channels exactly and neglecting the 2s channel entirely. In Fig. 2 (dashed curve) we have calculated $\sigma(2p)$ in a 1s–2p close-coupling calculation and to a first approximation it does represent the cross section reasonably well. The shape is a little wrong, with the cross section undershooting by about 20% at mid angles and being 50% too large in the backward direction. If we then put the 2s channel in approximately via the UBA (dotted curve) we note that the backward angle behaviour is improved noticeably. The omission of the real part of the Green function in the 2s channel is only significant in the 50°–90° region and leads to a lessening of the cross section there.

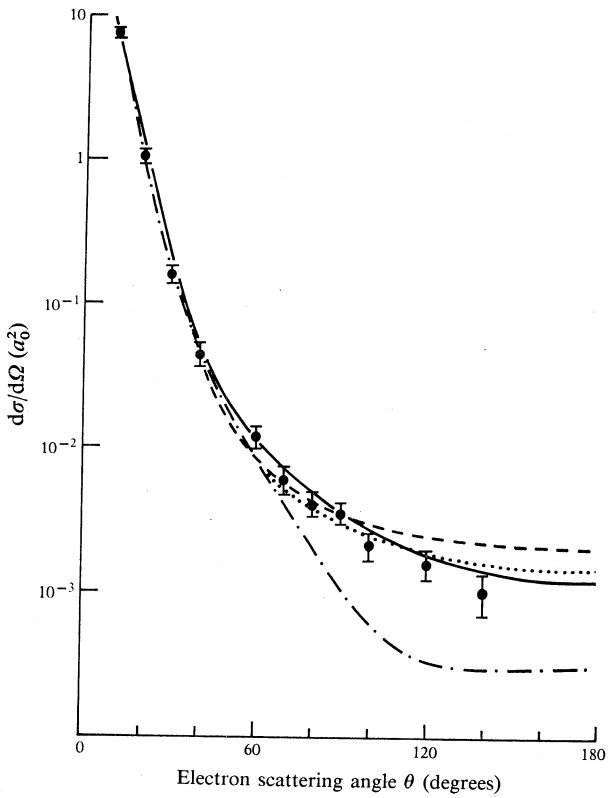

Fig. 2. Inelastic cross section $\sigma(2p)$ at $E = 54{\cdot}46$ eV calculated for four approximations: solid curve, 1s–2s–2p; dotted curve, 1s–2s(UBA)–2p; dot–dash curve, 1s–2s–2p(UBA); dashed curve, 1s–2p (two-state close coupling). The experimental results are from Williams (1981).

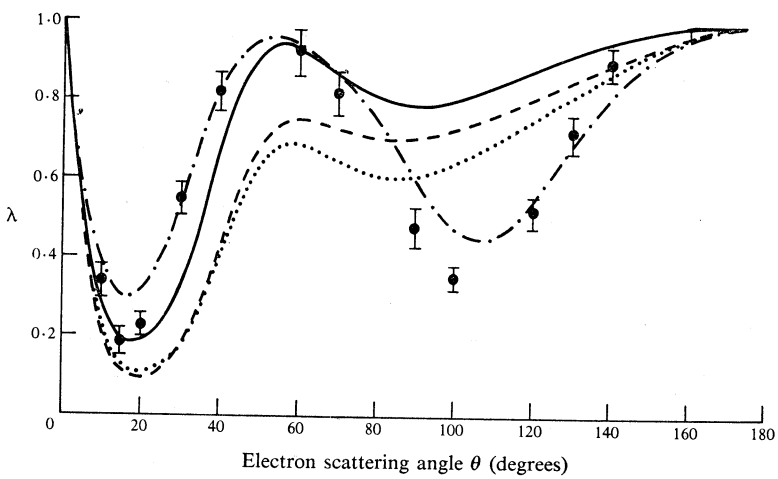

Fig. 3. Parameter λ at $E = 54{\cdot}46$ eV. (See caption to Fig. 2.)

Suppose now that we apply the UBA in the 2p channel but close couple the 1s and 2s states fully. Intuitively this approximation is more drastic, since we are approximating one of the channels explicitly involved in the transition. This is confirmed by the result in Fig. 2 (dot–dash curve), where the approximation of the 2p Green function has a drastic effect at backward angles. Thus it is evident that one really needs to take account of the off-shell scattering in the 2p channel properly. To carry this reasoning further we can similarly deduce that the 1s–2s cross section is also grossly in error unless the 1s and 2s channels are fully coupled. Thus, the simplest model one can resort to, in describing both $\sigma(2s)$ and $\sigma(2p)$ and including the significant reaction mechanisms, appears to be the full three-state close-coupling model.

The recent electron–photon coincidence experiments of Weigold *et al.* (1980) and Williams (1981) at 54·46 eV have provided us with more stringent tests of theory as they measure angular correlation parameters between the individual magnetic sublevels of the 2p state in 1s–2p transitions. The cross section $\sigma(2p)$ discussed above only gives us information over the summed levels. The correlation parameters can be measured in terms of the quantities λ and R defined as

$$\lambda = |T^{(0)}_{1s2p}|^2 \Big(\sum_{m=-1}^{+1} |T^{(m)}_{1s2p}|^2 \Big)^{-1},$$

$$R = \mathrm{Re}(T^{(0)}_{1s2p} T^{(1)}_{1s2p}) \Big(\sum_{m=-1}^{+1} |T^{(m)}_{1s2p}|^2 \Big)^{-1}.$$

In Fig. 3 we have plotted λ for an energy of 54·46 eV. The three-state close-coupling model (solid curve) is in fair agreement with experiment at forward angles but fails to reproduce the deep minimum in the backward direction. We note also that the λ parameter is more sensitive to approximation than $\sigma(2p)$. For instance the 1s–2p and 1s–2s(UBA)–2p models give a reasonable approximation to $\sigma(2p)$ in the three-state close-coupling model. The differences are highlighted in the λ parameter. If we look at the 1s–2p (dashed) curve we find that the effect of not including coupling to the 2s channel at all is to reduce the λ parameter (which is restricted to lie between 0 and 1) by up to 25% over a large range of the angles. The overall shape however remains fairly well intact. If we now couple in the 2s state via the UBA (dotted curve), perhaps surprisingly, there is worse disagreement with the three-state model at backward angles. At angles $\leqslant 40°$ there is no significant difference between the 1s–2p and 1s–2s(UBA)–2p. Since the latter includes more of the reaction mechanism than the former it shows that there must be considerable cancellation involved in the multiple-scattering series terms which are present when the 2s channel is taken fully into account. Most unexpectedly, the 1s–2s–2p(UBA) model (dot–dash curve), which gives a poor representation of $\sigma(2p)$, gives the best fit to the experimental data. If one compares it with the three-state model one sees that the coupling of the 2p channel via the principal value Green function is very significant in determining the shape of λ in the backward direction.

Disagreement between theory and experiment is further reinforced by looking at the R-parameter models in Fig. 4. The three-state close-coupling model (solid curve) is in accord with experiment for forward angles but disagrees badly at backward angles. Again the two models which do not include full coupling to the 2s states are in much worse disagreement with experiment. Coupling in the 2s state via the UBA makes only a small difference. The 1s–2s–2p(UBA) model (dot–dash curve)

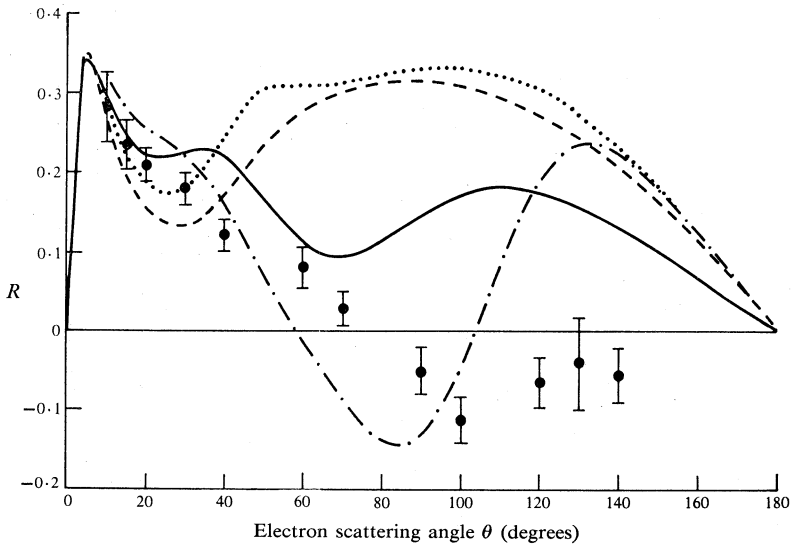

Fig. 4. Parameter R at $E = 54{\cdot}46$ eV. (See caption to Fig. 2.)

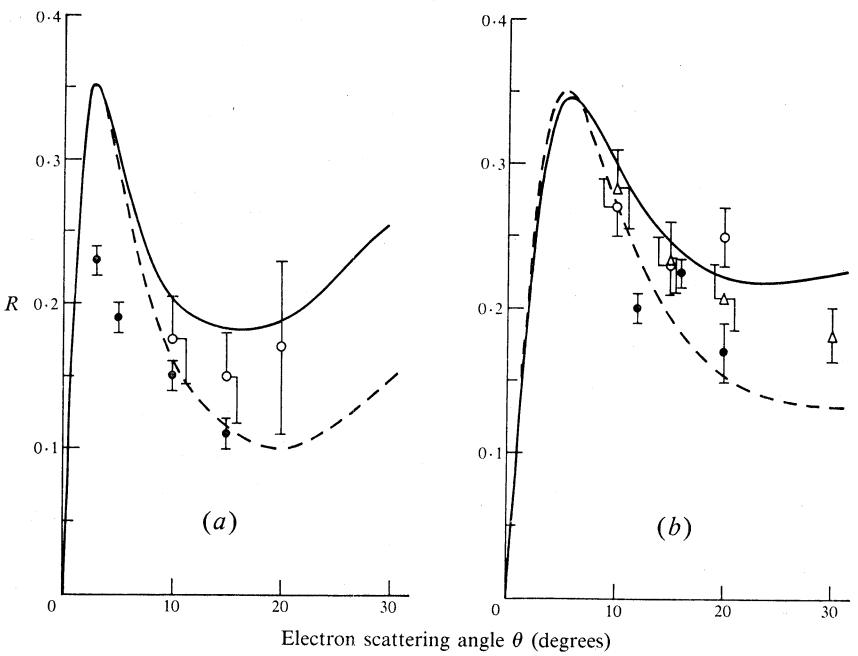

Fig. 5. Parameter R at an energy of (*a*) 100 eV and (*b*) 55 eV. Theory: solid curve, 1s–2s–2p (three-state close coupling); dashed curve, 1s–2p (two-state close coupling). Experiment: solid circles, Slevin *et al.* (1980); open circles, Hood *et al.* (1979); triangles, Williams (1981).

is the only one which is able to reproduce the sign change in R. Again we emphasize the marked effect of coupling to the 2p channel in an approximate way.

What can we conclude overall from the above study of the models for λ and R? Firstly, it is obvious that the three-state close-coupling model is inadequate to describe λ and R, although it does reproduce $\sigma(2p)$ well and also the ratio $\sigma(2s)/\sigma(2p)$. We

have seen that λ and R are very sensitive to the way the 2s state is coupled. It therefore suggests that coupling of the $n = 3$ levels will certainly be important. The fact that R seems more sensitive to approximation than λ leads us to suspect that possibly even higher levels may be needed to get R right.

Since the one region where experiment and theory are not too dissimilar is at forward angles, we shall conclude our analysis by looking at R in the forward direction. Even though experiments over the full angular range have not been performed above 54·46 eV, there are some results at 100 eV due to Hood *et al.* (1979) and Slevin *et al.* (1980). In Figs 5*a* and 5*b* we show experimental results at 100 and 55 eV respectively and compare them with the 1s–2p and 1s–2s–2p close-coupling results. It appears that coupling to the 2s channel becomes unimportant for angles less than 5° where there is a pronounced peak for both energies. The height of the peak seems independent of the energy, though it is much sharper at 100 eV. Below 20° the three-state model is in accord with the results of Hood *et al.* (1979) and Williams (1981). It is puzzling therefore that at 55 eV Slevin *et al.* (1980) predicted structure which neither theory nor other experiments find. Similarly at 100 eV their results predicted the sharp increase in R, but well below the theory results. Whereas our various models give different results at larger angles, the forward peak structure is not sensitive to the details of the models. Thus, it is difficult to see what mechanism could be added to the close-coupling models to bring them in better agreement with experiment.

6. Conclusions and Summary

We have analysed the approximations involved in elastic scattering at intermediate energies. For second-order models without closure we have estimated that errors in the approximations contribute at most 10% above 50 eV. All theories give shapes similar to experiment, but with significantly lower values at 100 eV. There is no such marked disagreement at 50 or 200 eV. We therefore concur with Kingston and Walters (1980) in suggesting that there is some need to have the experiment redone at 100 eV.

For inelastic scattering we have seen that the angular correlation parameters λ and R are much more sensitive to approximations in the reaction mechanism. There appears to be considerable cancellation between groups of terms in the multiple-scattering series. This indicates that close-coupling models will have to take into account states from higher levels to obtain satisfactory agreement with experiment.

At very forward angles there is disagreement between various experiments. Also, the experiments stop just short of the angular range where theory finds some structure. We would therefore welcome an experiment at 54·46 and 100 eV that either confirms or rejects the present calculations.

Acknowledgments

One of us (A.T.S.) would like to thank the Australian Research Grants Scheme for a Research Fellowship.

References

Burke, P. G., and Robb, W. D. (1975). *In* 'Advances in Atomic and Molecular Physics', Vol. 11, pp. 143–214 (Academic: New York).

Burke, P. G., and Schey, H. M. (1962). *Phys. Rev.* **126**, 147–62.

Burke, P. G., Schey, H. M., and Smith, K. (1963). *Phys. Rev.* **129**, 1258–74.

Burke, P. G., and Smith, K. (1962). *Rev. Mod. Phys.* **34**, 458.
Burke, V. M., and Seaton, M. J. (1961). *Proc. Phys. Soc. London* **77**, 199–212.
Byron, Jr, F. W., and Joachain, C. J. (1981). *J. Phys.* B **14**, 2429–48.
Faddeev, L. D. (1961). *Sov. Phys. JETP* **12**, 1014–19.
Fon, W. C., Berrington, K. A., Burke, P. G., and Kingston, A. E. (1981). *J. Phys.* B **14**, 1041–51.
Frost, L., and Weigold, E. (1980). *Phys. Rev. Lett.* **45**, 247–50.
Hood, S. T., Weigold, E., and Dixon, A. J. (1979). *J. Phys.* B **12**, 631–45.
Kingston, A. E., Fon, W. C., and Burke, P. G. (1976). *J. Phys.* B **9**, 605–18.
Kingston, A. E., and Walters, H. R. J. (1980). *J. Phys.* B **13**, 4633–61.
Lawson, J., Lawson, W., and Seaton, M. J. (1961). *Proc. Phys. Soc. London* **77**, 192–8.
McCarthy, I. E., Saha, B. C., and Stelbovics, A. T. (1981*a*). *Phys. Rev.* A **33**, 145–52.
McCarthy, I. E., Saha, B. C., and Stelbovics, A. T. (1981*b*). *J. Phys.* B **14**, 2871–93.
Mayers, D. F. (1974). *In* 'Numerical Solution of Integral Equations' (Eds L. M. Delves and J. Walsh), pp. 64–79 (Clarendon: Oxford).
Mott, N. F., and Massey, H. S. W. (1965). 'The Theory of Atomic Collisions', 3rd edn (Oxford Univ. Press: New York).
Redish, E. F. (1980). *Phys. Lett.* B **90**, 188–92.
Saha, B. C., Chaudhuri, J., and Gosh, A. S. (1976). *J. Phys. Soc. Jpn* **41**, 1716–23.
Scott, T., and Bransden, B. H. (1981). *J. Phys.* B **14**, 2277–89.
Slevin, J., Eminyan, M., Woolsey, J. M., Vassilev, G., and Porter, H. Q. (1980). *J. Phys.* B **13**, L341–5.
Sloan, I. H., and Moore, E. J. (1968). *J. Phys.* B **1**, 414–22.
Teubner, P. J. O., Lloyd, C. R., and Weigold, E. (1974). *Phys. Rev.* A **9**, 2552–8.
van Wingerden, B., Weigold, E., de Heer, F. J., and Nygaard, K. J. (1977). *J. Phys.* B **10**, 1345–62.
Weigold, E., Frost, L., and Nygaard, K. J. (1980). *Phys. Rev.* A **21**, 1950–4.
Williams, J. F. (1975*a*). *J. Phys.* B **8**, 1681–92.
Williams, J. F. (1975*b*). *J. Phys.* B **8**, 2191–9.
Williams, J. F. (1981). *J. Phys.* B **14**, 1197–1217.

Manuscript received 6 May, accepted 16 August 1982